Analyse QTL de la ramification du chêne pédonculé en utilisant la tomographie à rayon X

Ce chapitre a fait l'objet d'une publication dans le journal « Tree Genetics & Genomes ». Je propose ici une synthèse de l'article, en français et je l'enrichi par l'analyse d'un trait lié à la flexuosité du tronc, non présenté dans l'article.

2.1 Résumé

2.1.1 Contexte et objectifs

Une nouvelle méthode d'observation à l'intérieur du bois a été développée grâce à la tomographie à rayon X. Cette technologie permet de quantifier les traces de bourgeon et les nœuds de branche dans le tronc et de créer des traits des ramifications plus précis par rapport à ceux observés à l'extérieur des troncs. Des études génétiques de la ramification épicormique chez le chêne montrent que le contrôle génétique est modéré (Jensen et al. 1997; Savill and Kanowski 1993). En fait, le déterminisme génétique sur la branche séquentielle a déjà été étudié chez le peuplier (Bradshaw and Stettler 1995; Wu and Stettler 1998) et le pin (Shepherd et al. 2002), mais il y a très peu de littérature qui met en évidence le contrôle génétique sur la ramification épicormique chez les arbres forestiers. Le contrôle génétique du bourgeon latent a été seulement étudié chez le pommier (Segura et al. 2009). C'est ainsi la première fois qu'un déterminisme génétique a été mis en évidence pour la ramification épicormique chez les arbres et aussi pour la branchaison séquentielle chez le chêne.

Dans ce contexte, l'objectif de cette étude est de quantifier le contrôle génétique sur la ramification du chêne et caractériser l'architecture de ce déterminisme génétique sur les chromosomes du chêne pédonculé. Pour cela, nous avons (1) estimé la variation phénotypique de la ramification du chêne pédonculé, (2) analysé des QTL pour chaque trait phénotypé et (3) analysé les colocalisations des QTLs liés aux différentes traits de ramifications en terme de dénominateur physiologique commun.

2.1.2 Méthodologie

Cet article est basé sur les résultats apportés par un dispositif expérimental d'une famille de pleins frères, obtenu par une croissement interspécifique de chêne pédonculé. Les observations internes des troncs des arbres échantillonnés ont été réalisées grâce à la tomographie à rayon X sur 332 billons (2 copies de 166 génotypes) récupérés après une éclaircie dans ce site expérimental. Les traits liés aux différents types de ramification (bourgeon primaire, bourgeon secondaire, branche séquentielle, branche épicormique) ont été mesurés en interprétant les images scannées. Pour chaque trait, une analyse QTL a permis d'évaluer si la variation du trait est liée à la présence d'un ou plusieurs marqueurs moléculaires et ainsi déterminer des endroits (loci) sur la carte génétique associés à la variabilité du trait observé.

En plus des traits liés aux ramifications présentés dans l'article précité, nous avons aussi mesuré le trait lié à la flexuosité du tronc, quantifiée par la différence entre la longueur exacte de la moelle de tronc et la distance directe la plus courte du début à la fin de la moelle (dLC) de la portion de tronc.

2.1.3 Résultats principaux

Les traits de ramification variaient considérablement. Des QTLs fortement significatifs ont été détectés pour les traits liés aux bourgeons latents et aux branches épicormiques. Six QTLs ont été détectés pour le nombre de bourgeons latents, et ces QTLs expliquent entre 5,2% et 6,6% de la variation phénotypique. Cela montre que le contrôle génétique du bourgeon latent s'exprime par des petits effets sur plusieurs chromosomes. L'ensemble de ces QTLs explique au total environ 30% de la variation phénotypique, mais ce chiffre risque d'être surestimé à cause de seulement deux répétitions de chaque génotype et du nombre faible de génotypes. Les QTLs qui expliquent plus de 10% de la variation phénotypique sont principalement détectés pour le trait lié aux bourgeons primaires. Pour les autres types de rameaux latéraux, très peu de QTLs ont été détectés. Seulement un QTL a été repéré pour le nombre de branches séquentielles avec 8,3% de PEV. D'ailleurs, aucun QTL significatif pour les branches épicormiques et le bourgeon secondaire n'a été détecté. Pour le trait « pourcentage de branches épicormiques développées », 4 QTLs expliquent au total 27,5% de la variance phénotypique. En revanche, nous n'avons pas détecté de QTL lié à la flexuosité du tronc.

Cela confirme que l'effet génétique sur les bourgeons latents et le développement des branches épicormiques est relativement modéré. Le nombre de branches séquentielles n'est pas corrélé avec le volume total des branches séquentielles ni avec les autres types de ramification. Sur les chromosomes du chêne pédonculé, nous avons observé trois hot-spots qui regroupent les QTLs liés aux différents types de ramification.

2.1.4 Conclusions

Ces résultats montrent la possibilité de quantifier l'effet génétique et examiner l'architecture génétique liée à la ramification du chêne grâce à l'observation à l'intérieur du bois par tomographie à rayon X. Ces QTLs détectés montrent que le contrôle génétique des bourgeons latents et des branches épicormiques reste modéré. Le contrôle génétique de la branchaison séquentielle est indépendant de celui d'autres types de ramification, car aucune colocalisation de QTLs n'a été trouvée pour à la fois le nombre de branches séquentielles et les autres types de rameaux latéraux. Ces QTLs qui ont un petit effet allélique se répartissent sur la plupart des chromosomes du chêne. Par conséquent la sélection génétique en vue d'améliorer la qualité du bois en réduisant l'effectif de la ramification épicormique semble difficile à réaliser.

En revanche, sur certaines régions génomiques ont été mises en évidence des colocalisations des QTLs des bourgeons latents et des branches épicormiques. Le contrôle génétique de la ramification épicormique dans ces régions génomiques est probablement lié aux mécanismes de l'initiation du méristème axillaire et de la dormance du bourgeon.

Tree Genetics & Genomes (2017) 13:5
DOI 10.1007/s11295-016-1083-y

ORIGINAL ARTICLE

X-ray computed tomography to decipher the genetic architecture of tree branching traits: oak as a case study

Jialin Song[1] · **Oliver Brendel**[2] · **Catherine Bodénès**[3] · **Christophe Plomion**[3] · **Antoine Kremer**[3] · **Francis Colin**[1]

Received: 30 June 2016 / Revised: 14 November 2016 / Accepted: 29 November 2016

Abstract A new method for obtaining internal views of tree trunks was recently developed using X-ray computed tomography (CT). This technology makes it possible to observe and measure rameal traces that are left by latent buds, sequential branches, and epicormic branches in the wood. Epicormic branches are undesirable for producing high-value solid wood, especially in *Quercus robur*, an important hardwood forest tree species in Europe, which is prone to epicormic branches that develop from abundant latent buds. For the very first time, branching-related traits deduced from X-ray CT observation make it possible to analyze the genetic architecture of oak branching through a quantitative trait locus (QTL) analysis. Highly significant QTLs were detected for traits related to latent buds and epicormic branches. The number and effect of these QTLs suggest a moderate genetic determinism for the formation of latent buds and the development of epicormic branches. Three hotspots were found, grouping QTLs for different branching traits. An analysis of the common physiological denominators of these coincident traits suggests that their genetic controls are related to either the regulation of the axillary meristem initiation or to bud dormancy. Conversely, the position of only the separate QTL related to the number of sequential branches suggests an independent genetic control.

Keywords Pedunculate oak · Computed tomography · Epicormic · Latent bud · QTL

Communicated by D. Grattapaglia

Electronic supplementary material The online version of this article (doi:10.1007/s11295-016-1083-y) contains supplementary material, which is available to authorized users.

✉ Francis Colin
francis.colin@inra.fr

[1] LERFoB, INRA, AgroParisTech, 54000 Nancy, France

[2] EEF, INRA, Université de Lorraine, 54280 Champenoux, France

[3] BIOGECO, INRA, University of Bordeaux, 33610 Cestas, France

Introduction

Pedunculate oak (*Quercus robur* L.) is one of the most important hardwood tree species in Europe where it ranges from the north of Spain to Russia. In France, it is considered a dominant species, with over two million hectares of forest producing 7 million m^3 of timber/year (IGN 2013). Oak timber is graded according to four quality classes (A, B, C, and D), which are strongly correlated with timber values, with the price varying 100-fold from class D to A (Forêts de France 2015). Sprouts and related defects (Colin et al. 2010a) are important factors affecting wood quality in oak species, causing up to a 13% reduction in timber value, with an average downgrading of one class (Meadows and Burkhardt 2001). In addition, epicormic branches (that develop from the latent buds) are a particular concern in terms of obtaining higher timber values. With this in mind, several forest management practices were proposed by Colin et al. (2012).

Besides the external observation of latent bud structures, several methods have been developed to observe lateral traces inside the trunk of a tree. In a study by Fontaine et al. (2004), 1- to 2-mm-thick serial transverse sections were made on wood samples containing epicormic traces. However, this method was only efficient when epicormic structures could be externally observed. The development of non-invasive methods, including optical scanning and X-ray computer tomography (CT), make the 3D visualization and quantification of wood structure accessible (Colin et al. 2010a). In particular,

Published online: 14 December 2016

a new method was developed using X-ray computed tomography (Fig. 1), allowing accurate observations of all rameal traces, both knots and bud traces, inside wood samples, even when these knots and traces are no longer visible on the stem surface. This methodology highlighted a strong correlation between the number of epicormics at the bark surface and the number of bud traces and rameal sequences near the pith of young sessile oak trees (*Quercus petraea*) (Morisset et al. 2012a). This correlation suggested that epicormics are not only dependent on environmental factors such as soil fertility (Harmer 1989) and light exposure (Chaar and Colin 1999) but also on the ontogenesis, mainly influenced by the primary growth.

The height growth of the main stem of an oak tree is monopodial. It is also polycyclic, meaning that more than one growth unit (GU) can develop within an annual shoot (AS), depending on age and environment (Heuret et al. 2000; Nicolini et al. 2000). Within each GU, axillary bud meristems frequently initiate a few unexpanded leaves and then stop their growth, forming small axillary buds in the leaf axil (Leyser 2009). This axillary bud, referred to as the primary bud (PriBD; Table 1), may have one of the following fates (Fig. 2): (i) it may persist as a latent bud that may remain inactive for several years and present a horizontal bud trace in the wood (primary latent bud (PriLBD)); (ii) it may develop into a sequential branch (SeqBC) the following spring, producing a sequential knot in the stem; or (iii) it may develop into an epicormic branch (EpiBC) from the latent bud several springs later, producing an epicormic knot in the stem. Within the stem wood, an epicormic branch is easily recognizable by its epicormic knot pith that is not directly connected to the pith of the main stem but, instead, indirectly connected through the horizontal trace of a latent bud (Morisset 2012). In addition to axillary buds, (iv) a secondary bud (SecBD) can develop at the base of any of the previous buds or branches and produce a bud trace (Fontaine et al. 1999; Colin et al. 2008). Secondary buds can only develop into epicormic branches or persist as secondary latent buds (SecLBD). Here, we use the general term "lateral" to designate the four types of traces (A, B, C, and D, illustrated in Fig. 2) and "epicormics (Epis)" to designate latent buds (PriLBD and SecLBD) and EpiBC. Using X-ray computed tomography, rameal traces within the trunk wood can be observed, making it possible to estimate the volumes of sequential and epicormic knots and to derive traits related to both sequential and epicormic branching.

Only a few studies have reported genetic variations of epicormics. A narrow-sense heritability of 0.38 was calculated for the number of epicormic branches in a young, open-pollinated progeny trial of *Q. robur* and *Q. petraea* (Savill and Kanowski 1993). A higher narrow-sense heritability (h^2 = 0.57) was found for the same trait in a 19-year-old open-pollinated progeny trial of sessile oak (*Q. petraea*) (Jensen et al. 1997). Recently, the comparison between several half-sibs of 25-year-old *Quercus alba* showed that the families with fewer epicormic branches also had a lower number of epicormic traces and a higher number of latent bud traces, thereby suggesting genetic correlations among these traits (Meier and Saunders 2013). All together, these results strongly suggest that traits related to epicormic branches are under genetic control.

Furthermore, the analysis of the genetic architecture of branching-related traits, in terms of quantitative trait loci (QTL) would yield valuable knowledge to better understand their genetic determinism. Over the past 25 years, QTLs in forest trees were mainly focused on growth (poplar: Bradshaw and Stettled 1995; beech: Scalfi et al. 2004; eucalyptus: Freeman et al. 2013), bud phenology (poplar: Frewen et al. 2000; Fabbrini et al. 2012; oak: Scotti-Saintagne et al. 2004), and other adaptive traits (e.g., in oak, water use efficiency (Brendel et al. 2008); tolerance of waterlogging (Parelle et al. 2007); rooting ability (Scotti-Saintagne et al. 2005); and stomatal density (Gailing et al. 2008)). For sequential branching traits derived from external observations, QTLs underlying sylleptic and proleptic branching were detected in poplar (Bradshaw and Stettled 1995; Wu 1998). Branch number per whorl was studied in pine (Shepherd et al. 2002). In fruit trees, a small number of large-effect QTLs related to the total branch number was also detected in apple (Conner et al. 1998; Segura et al. 2008) and in apricot (Socquet-Juglard et al. 2012).

In the QTL study of apple tree architecture, Segura et al. (2008) reported that the QTLs of latent buds on the trunk were detected in the same chromosome. In fact, two QTLs were detected in a very close region and explained 22% and 23% of the phenotypic variance, respectively. To the best of our knowledge, this is the only study that has been carried out to elucidate the genetic architecture of epicormic branching traits. The CT methodology allows not only the derivation of branching-related traits inside the trunk, but the screening of a sufficiently high number of individuals required for a QTL analysis as well.

In this context, the objective of this study was 2-fold: (1) to estimate the phenotypic variation of branching traits in a full-sib family of pedunculated oak, using X-ray tomography as a new method for observing rameal traces within the trunk and (2) to analyze coincidences of QTLs for the different measured branching traits in terms of their underlying physiological determinants. For this purpose, we took advantage of a thinning made in a full-sib cross of pedunculate oak from which parental genetic linkage maps were recently established using SNP markers (Bodénès et al. 2016).

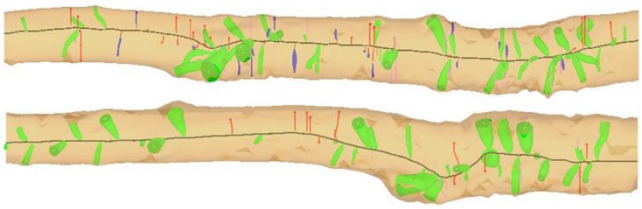

Fig. 1 3D reconstruction of two logs by Bil3D software. This 3D virtual image displays the pith of the log (in *black*) and the four lateral types (primary bud traces in *red*, sequential knots in *green*, epicormic knots in *blue*, and secondary bud traces in *pink*) inside the wood

Material and methods

Genetic material

We used a full-sib family of 166 offspring, which was obtained from an intraspecific cross of *Q. robur*. The male parent (accession A4) is located in a wooded parkland near Arcachon, France (44°40′N, 1°11′W); the female parent (accession 3P) is located at INRA's Pierroton Forest Research Station (44°44′N, 0°46′W). Rooted cuttings were produced from a clonal bank of 278F1s from which 207 genotypes (with approximately ten copies per genotype) were planted in 2000 in an INRA experimental site in southwestern France (Bourran: 44°20′N, 0°24′W). The clonal replicates of the mapped pedigree were planted according to a randomized incomplete block design (183 blocks with 12 cuttings each, for a total of 2196 individuals) (Saintagne et al. 2004). The replicates were planted 1.5 m apart in rows, and the rows were separated from each other by 4 m. During a systematic thinning in spring 2012, 1-m-long logs were recovered between 40 and 140 cm in height from two replicates of each of the 166F1s.

Genetic linkage map construction

High-density genetic linkage maps were established for both the 3P (female) and A4 (male) parents by Bodénès et al. (2016) using gene-based markers (SNP). A subset of SNP markers evenly distributed along the 12 linkage groups (LG) was selected in this study to reconstruct two new parental linkage maps for QTL analysis following the JoinMap procedure described in Bodénès et al. (2016). The male linkage map contains 341 markers and the female linkage map contains 345 markers (Table 2).

Table 1 List of the traits and their description

Lateral type	Trait	Description
Primary buds	nPriBD[a]	Number of total primary buds
	nPriLBD[a]	Number of primary buds having reached the bark
Sequential branches	nSeqBC[a]	Number of sequential branches
	vSeqBC[a]	Sum of sequential knot volume in 1 m (cm^3)
	aSeqBC	Mean inclination angle per log of the sequential branches (deg)
	nFork	Number of sequential branches with an inclination angle more than 45°
Epicormic branches	nEpiBC[a]	Number of epicormic branches
	vEpiBC	Sum of epicormic knot volume in 1 m (cm^3)
Secondary buds	nSecBD[a]	Number of secondary buds
Primary buds and sequential branches	nP[a]	Number of PriBD and SeqBC
All latent buds	nLBD[a]	Number of all of the buds having reached the bark (PriLBD and SecLBD)
Epicormics	nEpis[a]	Total number of all of the latent buds and epicormic branches (nLBD and EpiBC)
	rEpiBC	Ratio of nEpiBC to nEpis multiplied by 100 (%)

All numbers are per meter

[a] The traits were standardized per 1 m of log length

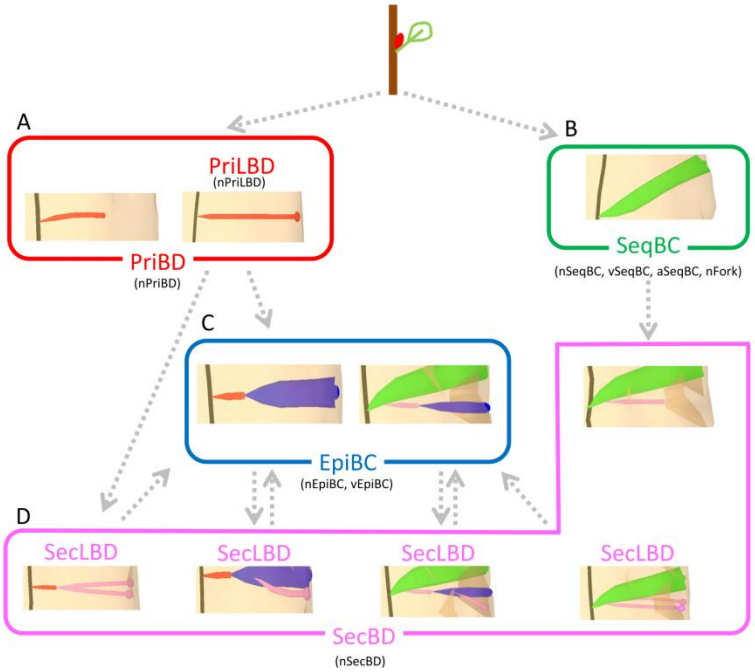

Fig. 2 Fate of an axillary bud (representation of the four lateral types developed from the axillary bud by 3D virtual imaging). The pith is in *black*, and the four lateral types are presented as follows: *A*, Primary bud (*PriBD*) traces in *red*. *Left*, a primary latent bud that has stopped developing; *right*, a primary latent bud that has reached the bark (*PriLBD*); *B*, sequential branches (*SeqBC*) in *green*; *C*, epicormic branches (*EpiBC*) in *blue*; and *D*, secondary bud (*SecBD*) traces in *pink*. *Upper right*, a secondary latent bud that has stopped developing. *Bottom*, secondary latent buds that have reached the bark (*SecLBD*). In each lateral type, a pinhead reflects the fact that the bud trace or the knot has reached the bark. The studied traits are indicated in *brackets below each lateral type* and presented in Table 1

Phenotyping by X-ray tomography

X-ray computed tomography (CT) has been recently used for internal observations of oak logs (Xylosciences Platform, INRA Nancy-Lorraine). The CT scans the logs by 2.5-cm-thick slices at a rate of 150 pictures/min. Woody materials are subject to X-ray attenuation due to their density and moisture. This is reflected by gray levels on the scan images: the denser and/or wetter the material, the brighter the image (Freyburger et al. 2007). Traces of four lateral types can be viewed (Fig. 3): (1) traces of primary latent buds, (2) knots of sequential branches, (3) knots of epicormic branches, and (4) traces of secondary latent buds.

All of the branching traces were manually marked by their successive positions on the scanned images using "Gourmand" (Freyburger et al. 2007), a plug-in developed under "ImageJ" open-source image-analysis software (http://rsbweb.nih.gov/ij/). Several files of these quantitative data were then created. One of these files is used by Bil3D software (Colin et al. 2010a) to reconstruct a virtual log in a 3D image (Fig. 1). Based on the manual interpretation of the scanned images, the following branching descriptors were quantified (Table 1): (1) the number of primary buds (nPriBD) and the number of primary buds having reached the bark (nPriLBD); (2) the number of sequential branches (nSeqBC), the total volume of sequential knots in 1 m (vSeqBC), the average of the inclination angle of the sequential branches (aSeqBC), and the number of sequential branches with an inclination angle >45° (nFork); (3) the number of epicormic branches (nEpiBC) and the total volume of

Table 2 Number of loci and size of the linkage groups

LG	3P		A4	
	Nb loci	LG size(cM)	Nb loci	LG size(cM)
LG1	31	52.5	26	54.4
LG2	46	84.2	46	102.4
LG3	22	53.4	25	61.3
LG4	26	57.8	17	63.7
LG5	35	61.6	31	70.1
LG6	27	52.1	30	62.7
LG7	27	50.9	24	57.8
LG8	30	61.8	32	66.8
LG9	26	56.8	26	56.2
LG10	21	54.7	29	58.2
LG11	24	50.4	29	59
LG12	30	50.7	26	56.1
Total	345	686.9	341	768.7

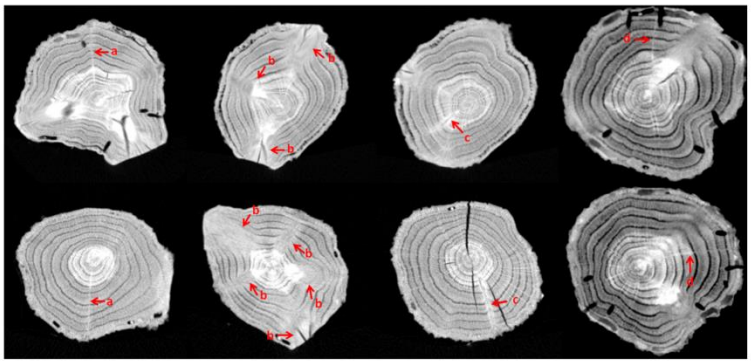

Fig. 3 Scanned images of a log showing the traces of the four lateral types: **a** primary latent buds, **b** sequential branches, **c** epicormic branches, and **d** secondary latent buds

epicormic knots in 1 m (vEpiBC); and (4) the number of secondary buds (nSecBD). The number of secondary buds having reached the bark (SecLBD) was not considered because most of the SecBD are maintained as secondary latent buds. Based on these descriptors, the following branching traits were calculated: the number of laterals directly related to the pith (nP), the number of latent buds on the bark (nLBD), the total number of epicormics (nEpis), and the ratio between the number of epicormic branches and the sum of epicormics (rEpiBC). All of the branching traits and the knot volume trait were standardized per 1 m of log.

Basic statistical analyses

The normality of the phenotypic values was visually inspected (Online resource 1). In the case where trait distribution strongly departed from normality, the trait value was log-transformed using a natural logarithm:

$$Z = ln(X + 1)$$

where Z is the transformed trait value and X the original trait value. "ln" was attached to the trait name for transformed traits.

The correlation matrix between all the traits (Online resource 2) was obtained with R (R Core Team 2015). The correlation network of the branching traits was performed with the "qgraph" R package (Epskamp et al. 2012). The phenotypic correlation analysis was also carried out with a dataset in which the outliers were removed. A similar result was obtained, showing that outlier data did not considerably influence the correlation structure.

The complete full-sib plantation was set up as a randomized incomplete block design. However, the samples used in this study were recovered from a thinning campaign. Therefore, the samples did not sufficiently represent the original block setup. Thus, to test a block effect a posteriori, the plantation was divided into seven blocks of similar size, with between 40 and 50 individuals in each. The main effects were estimated by two-way ANOVA, using the following linear model:

$$Y_{ij} = \mu + G_i + B_j + \varepsilon_{ij}$$

where Y_{ij} is the observed phenotypic value of the trait, μ the overall mean, G_i the genetic effect of genotype i, B_j the effect of block j, and ε_{ij} the error term.

A significant block effect was detected for the following traits: nPriBD, nPriLBD, vEpiBC, and rEpiBC. For each of these traits, the proportion of the variation explained by the block effect was calculated by the ratio of the sum of squares of the block effect to the total sum of squares. The part of the variation explained by the block effect was very low (ranging from 3% to 5%). In addition, the QTL detection did not show any difference between these traits adjusted by block effect and the same traits without adjustment. The artificial block effect B_j was thus omitted and the mean value for each genotype was used for QTL analysis.

QTL detection

The QTL detection software MultiQTL (University of Haifa, http://www.multiqtl.com/) was used considering a single-trait QTL model for each trait. The multiple-interval mapping method (MIM; Kao et al. 1999) with 500 to 1000 permutations was used to detect QTLs and their respective position (L), the allelic substitution effect (effect), the significance of detection at the linkage group level (p_C), and the percentage of explained variance (PEV). The mean and the standard deviation of the QTL positions (L_{BS} and L_{BS}_SD) as well as the 95 % confidence interval were calculated by bootstrap analysis with 1000 resamplings. Because the allelic phase was unknown in the mapping population, we could only compare the direction of allelic effects within chromosomes. A QTL

with a type I error at the linkage group level (p_C) below 5% and an allelic effect significantly different from zero (95% confidence interval not overlapping zero) was considered a "putative" QTL (but still statistically significant). For "highly significant" QTLs, a more stringent type I error at the genome level (p_G) below 5% was used. It was estimated as:

$$p_G = 1-(1-p_C)^{M/m}$$

where M is the total number of markers on the map and m is the number of markers in a given linkage group (Scotti-Saintagne et al. 2004).

Only "highly significant" QTLs are presented in the "Results". Putative QTLs will only be presented when they are co-localized with hotspots of highly significant QTLs. A multivariate QTL analysis of highly correlated traits (Korol et al. 1998) was carried out using the multi-trait approach of the MultiQTL software.

The graphical representation of the linkage groups and QTL positions was drawn with MapChart software (Voorrips 2002), using four QTL positions: (1) the position estimated by MIM (L); (2) the position calculated by bootstrap (L_{BS}); and (3) the two positions corresponding to the limits of the confidence interval at 95% calculated by bootstrap. To compare the position of QTLs detected on the male and female map, the composite genetic linkage map constructed by Bodénès et al. (2016) was loaded into Biomercator V3.0 (Sosnowski et al. 2012). The detected QTLs were projected on this composite map.

Results

Phenotypic variability and correlation structure

We found an average of 26.8 primary latent buds, 33.9 sequential branches, 29.9 epicormic branches, and 14.1 secondary latent buds/m (Table 3). On average, around 60% of the primary branching was sequential branches. A total of 19.4% of the latent buds led to epicormic branches, and over 80% of the epicormics were latent buds. A high level of variation was observed for all of these traits among the 332 logs recovered from the 166 genotypes. For instance, the number of primary buds ranged between 2.8 and 68.1, while the number of epicormics ranged between 6.6 and 189.8. All branching traits considerably varied except those related to sequential branches: nSeqBC, aSeqBC, and nP showed the lowest coefficient of variation (<30%) compared with the other branching traits (>40%).

Strong correlations were found for traits related to primary buds (nPriBD, nPriLBD, nP, nLBD_ln, and nEpis) with $R^2 > 0.5$ (Fig. 4). These five traits were combined to carry out a multi-trait QTL analysis (MUTLI5). Furthermore, nSecBD_ln, nLBD_ln and nEpis, related to secondary buds, were also strongly correlated among each other ($R^2 > 0.75$), and were thus also combined for a multi-trait analysis (MULTI3).

There was no correlation between any of the traits related to sequential branches and all the other branching types (Fig. 4). There was also no correlation between the nSeqBC and the vSeqBC, whereas the nEpiBC was correlated with the vEpiBC ($R^2 = 0.38$). The only correlation within the sequential branch trait is between the nSeqBC and the mean aSeqBC. However, this correlation was quite low ($R^2 = 0.18$).

Genetic architecture of branching traits

A total of 29 highly significant QTLs were detected among 61 putative QTLs distributed on five linkage groups (LG3, LG4, LG6, LG8, and LG11) for the female and on five LGs (LG1, LG3, LG6, LG7, and LG8) for the male. We found at least one putative QTL on each linkage group (LG), either on the female or on the male map. Each highly significant QTL explained from 5.2% to 11% of the phenotypic variance (Table 4). Most QTLs were detected for nLBD (i.e., six QTLs for the number of all of the buds having reached the bark), followed by nPriLBD (i.e., four QTLs for the number of primary buds having reached the bark). Both traits also showed the highest total percentage of explained variance for the highly significant QTLs detected (>30%). Four highly significant QTLs were also found for nFork, nEpis, and rEpiBC.

Regarding PriBD, two highly significant QTLs were detected for nPriBD on LG 6F with a positive allelic effect (Table 4), and on LG 7M with a negative effect. These two QTLs explained 9.1% and 10.8% of the PEV, respectively. For nPriLBD, a trait highly correlated with nPriBD, from 5.6% to 10.3% of the PEV was explained by four highly significant QTLs. These QTLs presented a negative effect on LG 3F, 11F, and 7M, and a positive effect on LG 6F.

Regarding sequential branches (SeqBC), only one highly significant QTL was detected with a PEV of 8.3% (Table 4), and this QTL did not co-localize with any other QTLs. Only one of three QTLs of aSeqBC was highly significant, with 9.8% of the PEV. It was located on LG 6M. For the trait "nFork," which quantifies the number of sequential branches with a small branching angle, four highly significant QTLs were detected, explaining from 5.5% to 8.1% of the PEV on LG 3F, 4F, 6F, and 8M, respectively.

Regarding EpiBC and SecBD, only one QTL for vEpiBC was highly significant, with 9.3% of the PEV on LG 11F (Table 4). No highly significant QTL was detected for nEpiBC and nSecBD.

For the trait nEpis, which was calculated by adding the epicormic branch number and the latent bud number, highly

Table 3 Descriptive statistics of tree branching traits based on untransformed assessment data

Lateral type		Mean	SD	Min	Max	CV
Primary buds	nPriBD	26.8	12.6	2.8	68.1	0.47
	nPriLBD	19.3	10.2	1.1	59.3	0.53
Sequential branches	nSeqBC	33.9	7.8	14.5	64.2	0.23
	vSeqBC	240.1	135.0	9.5	738.4	0.56
	aSeqBC	17.8	4.7	4.0	29.5	0.26
	nFork	2.1	1.6	0.0	8.0	0.75
Epicormic branches	nEpiBC	9.8	7.2	0.0	48.9	0.73
	vEpiBC	3.4	3.8	0.0	27.8	1.12
Secondary buds	nSecBD	14.1	14.4	0.0	118.2	1.02
Primary buds and sequential branches	nP	58.4	13.4	31.2	104.4	0.23
All latent buds	nLBD	29.9	19.6	1.7	148.0	0.66
Epicormics	nEpis	50.7	28.6	6.6	189.8	0.56
	rEpiBC	19.4	9.3	0	45.1	0.47

For the abbreviations and units, see Table 1

SD standard deviation, *CV* coefficient of variation

significant QTLs were both observed on the male and female maps of LG 6 (Table 4). On LG 7M, the QTL of nEpis had the highest contribution to the PEV in this study (11%), with a negative effect. For rEpiBC, which represents the proportion between nEpiBC and nEpis, four highly significant QTLs explained from 5.2% to 9.1% of the PEV. Two of them were observed on the male and female maps of LG 3 (Online resource 3) and had a positive effect; the other two were located on LG 1M and 8M, respectively, and presented a negative effect.

Hotspots between QTLs

QTL hotspots were mainly observed on LG 6, 7, and 8 (Fig. 5). These QTL co-localizations were expected since a significant phenotypic correlation was initially observed between these traits.

From the composite map, it can be seen that co-localized QTLs on the male and female maps on LG 7 were concentrated in a small homologous genomic region (Online resource 4), with traits related to primary buds, whereas for LG 6 and 8, the

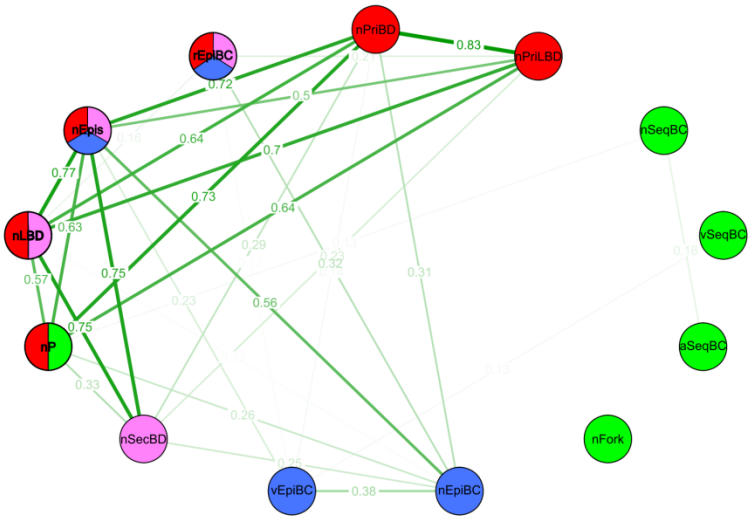

Fig. 4 Phenotypic correlation network for tree branching traits. *Node colors* indicate lateral type-related traits: primary buds (*red*), sequential branches (*green*), epicormic branches (*blue*), secondary buds (*pink*), and combination traits (*multicolor*, each color corresponds to the combination of lateral types). *Lines* connecting nodes represent significant correlations between traits ($p < 0.05$). The coefficients of determination are presented with a *green line*. *Line thickness* reflects the magnitude of the coefficients of determination

Table 4 QTLs of tree branching traits detected with single-trait analysis in the full-sib family of **Quercus robur** (3P × A4)

Lateral type	Trait	LG	MAP	LOD	PEV	Effect	L_{BS}	L_{BS}_SD	L	p_G
Primary buds	**nPriBD**	**6**	**F**	**4.12**	**9.1**	**6.1**	**12.71**	**10.20**	**10.39**	**0.0006**
	nPriBD	6	M	1.67	3.9	4.0	45.32	15.90	59.89	0.4290
	nPriBD	7	F	1.77	3.8	−3.9	10.75	10.10	9.78	0.3615
	nPriBD	**7**	**M**	**4.11**	**10.8**	**−6.7**	**8.60**	**6.40**	**6.49**	**0.0007**
	nPriBD	8	F	2.89	6.3	5.0	15.41	11.10	10.02	0.2073
	nPriBD	11	F	2.63	5.9	−4.9	5.81	7.70	2.60	0.1345
	nPriLBD	**3**	**F**	**2.80**	**5.6**	**−3.8**	**30.74**	**7.40**	**35.69**	**0.0008**
	nPriLBD	**6**	**F**	**4.99**	**10.3**	**5.2**	**12.67**	**8.00**	**10.39**	**0.0006**
	nPriLBD	7	F	1.76	3.4	−3.0	10.96	10.40	9.78	0.4009
	nPriLBD	**7**	**M**	**3.94**	**10.2**	**−5.0**	**7.60**	**4.70**	**6.28**	**0.0007**
	nPriLBD	8	F	2.58	5.1	3.6	13.73	9.20	10.03	0.1091
	nPriLBD	8	M	2.83	6.8	4.1	41.06	8.40	47.61	0.0520
	nPriLBD	**11**	**F**	**3.43**	**6.9**	**−4.2**	**3.47**	**6.50**	**2.17**	**0.0007**
Sequential branches	**nSeqBC**	**1**	**M**	**2.99**	**8.3**	**3.2**	**17.45**	**6.80**	**15.46**	**0.0006**
	nSeqBC	12	F	1.72	4.7	−2.4	12.16	11.00	11.74	0.2955
	vSeqBC	4	F	1.89	4.6	−46.4	7.37	10.60	1.24	0.3325
	vSeqBC	10	F	2.86	7	−57.2	4.44	9.70	0.00	0.0790
	vSeqBC	10	M	2.62	7.3	−59.2	49.07	14.90	58.22	0.1115
	aSeqBC	6	F	2.27	6.3	−1.6	39.38	8.80	37.29	0.2764
	aSeqBC	**6**	**M**	**3.78**	**9.8**	**−2.0**	**33.94**	**6.30**	**36.38**	**0.0006**
	aSeqBC	8	M	2.76	6.7	1.7	42.10	14.50	38.34	0.0520
	nFork_ln	**3**	**F**	**2.83**	**6.7**	**0.2**	**34.16**	**5.60**	**34.60**	**0.0008**
	nFork_ln	**4**	**F**	**3.50**	**8.1**	**−0.2**	**27.02**	**8.90**	**25.96**	**0.0006**
	nFork_ln	**6**	**F**	**2.40**	**5.5**	**−0.2**	**44.94**	**13.70**	**52.14**	**0.0499**
	nFork_ln	**8**	**M**	**2.67**	**6.8**	**0.2**	**40.08**	**13.30**	**32.47**	**0.0005**
Epicormic branches	nEpiBC_ln	1	F	2.36	6.3	0.3	38.98	10.70	45.99	0.1548
	nEpiBC_ln	7	M	2.23	6.1	−0.3	13.66	11.60	8.31	0.1932
	vEpiBC_ln	6	M	1.79	4.8	0.2	50.21	11.80	61.43	0.4061
	vEpiBC_ln	**11**	**F**	**3.51**	**9.3**	**−0.3**	**10.17**	**5.10**	**12.98**	**0.0007**
Secondary buds	nSecBD_ln	1	F	2.63	6.1	0.4	43.00	7.10	45.99	0.2014
	nSecBD_ln	2	M	2.14	5.2	−0.4	33.61	34.30	10.13	0.1060
	nSecBD_ln	5	F	1.54	3.5	0.3	17.57	12.10	12.71	0.3026
	nSecBD_ln	6	F	2.24	5.3	0.4	40.11	12.20	39.14	0.1756
	nSecBD_ln	6	M	1.70	4	0.3	39.16	11.90	42.30	0.1080
	nSecBD_ln	7	M	2.64	6.5	−0.4	18.45	14.60	6.35	0.0687
	nSecBD_ln	8	F	1.92	4.4	0.3	19.86	13.40	21.45	0.2526
Primary buds + sequential branches	nP	2	M	2.17	5.2	−4.8	19.50	29.90	2.71	0.1391
	nP	**6**	**F**	**3.65**	**7.7**	**6.0**	**15.89**	**13.90**	**10.39**	**0.0006**
	nP	7	F	2.58	5.3	−5.0	10.23	9.00	9.78	0.0620
	nP	7	M	2.67	6.7	−5.5	14.96	13.90	7.65	0.0554
	nP	**8**	**F**	**2.85**	**6**	**5.3**	**13.52**	**10.10**	**9.42**	**0.0006**
	nP	11	F	2.36	5	−4.8	8.48	11.30	2.67	0.1345
	nP	11	M	1.89	4.5	−4.5	12.27	16.00	5.57	0.4195

Table 4 (continued)

Lateral type	Trait	LG	MAP	LOD	PEV	Effect	L_{BS}	L_{BS}_SD	L	p_G
All latent buds	**nLBD_ln**	**1**	**M**	**2.70**	**6.5**	**0.3**	**41.74**	**14.30**	**52.24**	**0.0006**
	nLBD_ln	3	F	1.76	4.2	−0.2	28.91	12.30	38.36	0.4234
	nLBD_ln	**3**	**M**	**2.98**	**6.3**	**−0.3**	**2.56**	**9.50**	**0.00**	**0.0007**
	nLBD_ln	**6**	**F**	**2.47**	**6.1**	**0.3**	**38.91**	**14.80**	**52.14**	**0.0006**
	nLBD_ln	6	M	1.95	4.1	0.2	49.98	14.10	60.37	0.1578
	nLBD_ln	**7**	**M**	**3.04**	**6.6**	**−0.3**	**9.39**	**7.40**	**8.68**	**0.0007**
	nLBD_ln	**8**	**F**	**2.60**	**6.5**	**0.3**	**13.60**	**11.90**	**8.11**	**0.0006**
	nLBD_ln	**8**	**M**	**2.50**	**5.2**	**0.3**	**45.89**	**9.60**	**47.61**	**0.0005**
Epicormics	**nEpis**	**6**	**F**	**2.25**	**5.3**	**10.7**	**33.84**	**18.50**	**49.97**	**0.0499**
	nEpis	**6**	**M**	**3.17**	**7**	**12.2**	**43.94**	**11.60**	**37.33**	**0.0006**
	nEpis	**7**	**M**	**4.74**	**11**	**−15.3**	**7.35**	**4.20**	**7.23**	**0.0007**
	nEpis	**8**	**F**	**2.97**	**7.5**	**12.7**	**20.91**	**10.10**	**19.16**	**0.0006**
	nEpis	9	M	2.62	5.9	11.2	46.08	8.20	48.00	0.0759
	rEpiBC	**1**	**M**	**2.41**	**5.2**	**−3.3**	**34.76**	**11.40**	**31.23**	**0.0259**
	rEpiBC	**3**	**F**	**2.57**	**7**	**3.9**	**27.92**	**9.20**	**27.70**	**0.0309**
	rEpiBC	**3**	**M**	**4.21**	**9.1**	**4.4**	**9.24**	**5.30**	**9.57**	**0.0007**
	rEpiBC	5	F	2.21	5.5	−3.4	31.91	15.50	21.66	0.1969
	rEpiBC	**8**	**M**	**2.94**	**6.2**	**−3.7**	**47.26**	**11.00**	**51.94**	**0.0005**

The rows in italics are for highly significant QTLs; the other rows are for putative QTLs

MAP genetic map, *F* female map, *M* male map, *LG* linkage group, *L* position of the QTL on LG in centimorgans, *LOD* LOD score (log10 likelihood ratio comparing the hypothesis that there is a QTL at the marker with the hypothesis that there is no QTL anywhere in the genome), *PEV* percentage of variance explained by a QTL, *N* number of genotypes, *Effect* allelic effect (the unit of an effect is the unit of the trait which are mentioned in Table 1, for log-transformed traits, the units are also log-transformed), L_{BS} position of QTL calculated from bootstrap, L_{BS}_SD position of standard deviation for QTL calculated from bootstrap, p_G significance level at the genome level

QTLs detected on the female and male maps were found in distinct genomic regions. Indeed, two separate QTL clusters were observed on LG 6F as well as on LG 8F (Fig. 5): one cluster was composed of QTLs co-localized for traits of primary branching (nPriBD, nPriLBD, and nP), and another cluster was composed of QTLs for traits of secondary buds (nSecBD) or nEpis.

Surprisingly, the QTLs for the aSeqBC, a trait that was uncorrelated with the other branching traits, showed a close position with secondary bud traits on LG 6 and with primary bud traits on LG 8 (Online resource 4).

Multi-trait QTL analysis

For the MULTI5 model, which combined the traits related to the primary buds, one QTL was highly significant at the genome-wide level on LG 7M (Table 5). This highly significant QTL, which has significant allelic effects for all five traits, showed slightly higher PEV and allelic effects compared with those of single-trait analysis. In addition, this QTL was co-localized with the QTLs of five traits detected by the single-trait analysis (Fig. 5). Another QTL from the MULTI5 analysis was detected on LG 6F, which also exhibited significant allelic effects for all five traits and showed very similar PEV and allelic effects compared with those five highly significant QTLs detected by the single-trait analysis. However, this QTL was not significant at the genome-wide level and its position was not co-localized with the QTL cluster for the traits related to the primary buds (nPriBD, nPriLBD, and nP) on LG 6F.

For the MULTI3 model, no highly significant QTL was detected. The only putative QTL that has significant allelic effects for all three traits was barely significant at the genome-wide level (p_G = 0.0554). This QTL presented 7.7%, 6.6%, and 11% PEV for nSecBD_ln, nLBD_ln, and nEpis, respectively. It co-localized with the QTLs from the single-trait analysis and the highly significant QTL from the MULTI5 model on LG 7M (Fig. 5).

Discussion

Causal relationship between primary buds and epicormics

A large phenotypic variation was found for latent buds and epicormic branches within the *Q. robur* family analyzed. This

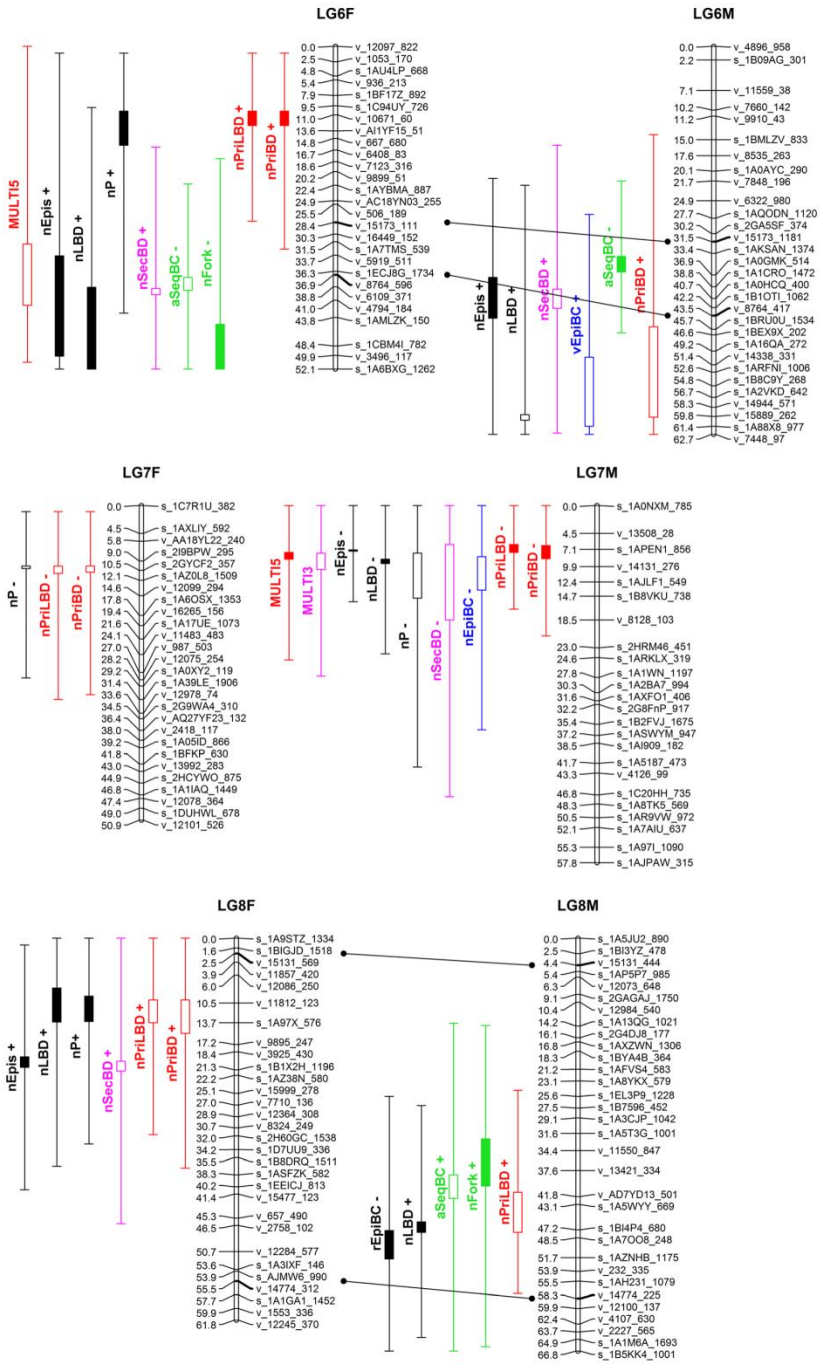
LG6F
LG6M
LG7F
LG7M
LG8F
LG8M
MULTI5
nEpis +
nLBD +
nP +
nSecBD +
aSeqBC -
nFork -
nPriLBD +
nPriBD +
vEpiBC +
nP -
nPriLBD -
nPriBD -
MULTI3
nEpis -
nLBD -
nSecBD -
nEpiBC -
rEpiBC -

Fig. 5 Female and male genetic linkage maps with the results of QTL detection superimposed. *Bar colors* indicate lateral type-related traits: primary buds (*red*), sequential branches (*green*), epicormic branches (*blue*), and secondary buds (*pink*). *Black bars* indicate the combined traits. *Full bars* represent highly significant QTLs; *empty bars* are putative QTLs; *positive* and *negative signs* indicate positive or negative allelic effects; *lines* connect orthologous SNP markers between both parental linkage groups

could be due to the low density of plantation that may have brought light to all the trees. We found a strong relationship between latent buds and epicormic branches. Colin et al. (2010b) also reported that the majority of epicormics found on the recently-formed annual shoots were latent buds. A similar result was shown in our study despite the greater age of the annual shoots investigated: about 80% of the epicormics were latent buds. We found that the number of primary buds and sequential branches (nP) was significantly correlated with the nLBD ($R^2 = 0.57$), which means that the higher the number of primary buds and sequential branches, the more latent buds that were observed on the bark. These latent buds can later develop into epicormic branches depending, for example, on future environmental conditions, water availability, light exposure, and damage (Morisset et al. 2012b). For epicormic branches, conversely to sequential branches, the number and total volume were correlated. This is probably due to the fact that the epicormic knots all have a relatively equivalent individual volume so that the volume strongly depends on the number, whereas the individual volume of sequential knots varies considerably since the branches in the upper part of each growth unit are thicker than those in the lower part. This suggests that the volume of knots was slightly more constant in epicormic branches than in sequential branches.

Important genetic determinism for axillary meristem initiation

On LG 7M, we found a hotspot with seven QTLs, all with a negative allelic effect. The presence of this cluster has to be related to the strong correlation within all branching traits except traits related to sequential branching. Using multi-trait QTL analysis, we found that the highly significant QTLs of the primary bud-related traits (MULTI5) co-localized with the putative QTLs of secondary bud-related traits (MULTI3). We assume that this coincidence is related to a common genetic control of bud production. Bud production depends on two phenomena: (1) the formation of the axillary meristem that begins at the time of leaf initiation from the primary shoot apical meristem and (2) the formation of an axillary bud from this axillary meristem (McSteen and Leyser 2005). These axillary buds may reactivate, growing out to form sequential branches in the same season or after a winter or growing out to form epicormic branches after several winters. On the basis of the CT observation of the bud traces or branch knots within the trunk, our branching traits directly represent the formation of an axillary meristem. Consequently, we suggest that the genetic control of bud production could be related to axillary meristem initiation.

On LG 6F, the QTLs for primary buds did not co-localize with QTLs for the strongly correlated traits such as the nEpis and nLBD. This result is coherent with that of the MULTI5 model from which no significant QTL at the genome-wide level was detected, even though all five QTLs detected by the single-trait analysis were highly significant. This suggests the presence of two different genetic mechanisms controlling latent bud production on LG 6F. One was found at the position of a QTL cluster for primary bud traits related to the axillary meristem initiation (see our assumption above for LG 7M). Another one was found at the position of a QTL cluster for latent buds and epicormics, where a putative QTL of nSecBD was also detected. This suggests that this second genomic region may carry genes involved in the regulation of bud initiation of the primary branching. Unfortunately, this genomic region could not be confirmed by our QTL analysis because no highly significant QTL of nSecBD were detected, although we found some putative QTLs of nSecBD co-localized with highly significant QTLs of primary buds in the other region.

The reason why we only detected some putative QTLs of nSecBD could be due to the fact that the number of secondary buds was primarily related to the number of sequential branches inserted just below the upper growth unit limit (Colin et al. 2010a). We could therefore assume that if the nSecBD trait had been standardized by annual shoot or growth units, these QTLs could have been detected and would have been highly significant. To test this hypothesis, an accurate detection of annual shoot limits would be necessary, which is not possible due to methodological reasons.

Common physiological denominator of epicormic branching traits: bud dormancy

As Meier et al. (2012) reported, the estimate of the number of epicormic branches at a given time may not be the best trait for assessing genetic control on epicormic dynamics since the interaction of genetics and environment could introduce unexpected variations. This may explain why no highly significant QTL was detected for the nEpiBC. However, we detected four highly significant QTLs for the rEpiBC. This suggests that the genetic control of the epicormic branch number was mediated by the regulation of the development of the latent buds into epicormic branches. In epicormic branch development, this genetic control of epicormic branches could be related to the regulation of bud dormancy and bud elongation. Since it is well known that axillary meristem initiation and bud dormancy are

Table 5 QTLs of tree branching traits detected with multi-trait analysis in the full-sib family of **Quercus robur** (3P × A4)

Trait	LG	MAP	LOD	PEV				Effect				L_{BS}	L_{BS_SD}	L	p_G
				nPriBD	nPriLBD	nP	nLBD_ln	nEpis	nPriBD	nPriLBD	nP	nLBD_ln	nEpis				
Multi5	6	F	4.20	9.2 **(9.1)**	10 **(10.3)**	7 **(7.7)**	5.6 **(6.1)**	4.8 **(5.3)**	6.15 **(6.1)**	5.02 **(5.2)**	5.83 **(6.0)**	0.30 **(0.3)**	10.8 **(10.7)**	31.9	16.4	41.8	0.1205
Multi5	**7**	**M**	**5.75**	**13.6 (10.8)**	**10.8 (10.2)**	**8.9** (6.7)	**9.6 (6.6)**	**12.1 (11)**	**−7.55 (−6.7)**	**−5.84 (−5.0)**	**−6.38** (−5.5)	**−0.36 (−0.3)**	**−16.4 (−15.3)**	**8.7**	**8.3**	**7.6**	**0.0280**

Entries set in italics are for highly significant QTLs; the others are for putative QTLs. The number in enclosed in parentheses refers to the results that were in single-trait analysis

MAP genetic map, *F* female map, *M* male map, *LG* linkage group, *L* position of the QTL on LG in centimorgans, *LOD* LOD score (log10 likelihood ratio comparing the hypothesis that there is a QTL at the marker with the hypothesis that there is no QTL anywhere in the genome), *PEV* percentage of variance explained by a QTL, *N* number of genotypes, *Effect* allelic effect (the unit of an effect is the unit of the trait which are mentioned in Table 2, for log-transformed traits, the units are also log-transformed), L_{BS} position of QTL calculated from bootstrap, L_{BS_SD} position of standard deviation for QTL calculated from bootstrap, p_G significance level at the genome level

related to plant hormones such as auxins, cytokinins, and strigolactones (Chatfield et al. 2000; Meier et al. 2012; Teichmann and Muhr 2015), a better understanding of the underlying molecular determinants of epicormic traits could be gained by studying whether or not the QTLs are enriched in genes involved in plant hormone biosynthesis and regulation. The oak genome sequence (Plomion et al. 2016) will provide more insights into this new research direction.

Independent genetic control for traits related to sequential branching

The homogeneity of the number of sequential branches per meter (around 20 sequential branches/m of main stem) in *Q. petraea* and *Q. alba* reported by Morisset et al. (2012a) and Meier and Saunders (2013) was not found in our study. Instead, we found a much higher number of sequential branches: an average of 33.9/m. This larger number could be merely due to the different species studied (*Q. robur* vs. *Q. petraea* and *Q. alba*), to the diversity created by a large full-sib family, or to technical differences during image interpretation. In fact, compared with the 28- to 55-year-old trees in the previous study, epicormic branches with very short latent bud traces may have been considered sequential branches in the young trees measured in the present study (14 years old).

Concerning sequential branches, only one highly significant QTL was detected for nSeqBC. Similar results were obtained in fruit trees: two QTLs were detected for the branch number, contributing to 7.1% and 24.3% of the PEV, respectively, in 3-year-old apple trees (N = 172; Conner et al. 1998). In apricot, 14.6% of the PEV was represented by one QTL for the total number of branches (N = 101; Socquet-Juglard et al. 2012). For Pinus, three QTLs were detected for the branch number per whorl, with 12–18% of the PEV (N = 89; Shepherd et al. 2002). The QTL of nSeqBC was not co-localized with any QTL of other branching traits, not even with the QTL for the vSeqBC. We assumed that the genetic control of the number of sequential branches was independent of other branching traits. Compared with previous QTL studies for branching traits, more complete branching traits have been investigated here thanks to within trunk observations, thus improving our understanding of tree branching genetic architecture.

For the aSeqBC, one highly significant QTL was detected and at a position close to the other branching traits, while in *Pinus*, there was no QTL detected for the average branch angle (Shepherd et al. 2002), and six QTLs for sylleptic branch angle were detected in poplar,

the PEV of each QTL ranged from 7.4% to 12.8% (Zhang et al. 2006).

Effect and architecture of the QTLs detected

Darvasi and Soller (1997) showed that the sampling size of the experiment is an important parameter for QTL detection, where detection is more accurate with a larger population. Indeed, our number of genotypes, limited to 166, reduced the statistical power of QTL detection. As a direct consequence, the PEV values of the QTLs are certainly overestimated by a factor of two or three (Beavis 1994). This was the reason why we performed a multi-trait analysis. The results of the multi-trait QTL analysis showed that the LOD score, the position and the effect of only the highly significant QTLs were refined. Nevertheless, it was surprising to note that the PEV contributed by each trait was slightly higher than the one found from the single-trait analysis.

We detected four highly significant QTLs with percentages of variance above 10%. In studies with a comparable number of genotypes analyzed, ten QTLs related to rooting ability were detected with PEVs varying from 4.3% to 13.8% (N = from 138 to 213; Scotti-Saintagne et al. 2005). The following studies all used a multi-environment model, increasing the QTL detection power: QTLs related to bud burst were detected, explaining from 3% to 11% of the PEV (N = from 89 to 216; Scotti-Saintagne et al. 2004); QTLs related to waterlogging response and root hypoxia were also detected, explaining from 2.9% to 20.6% of the PEV (N = 120; Parelle et al. 2007); QTLs detected for water use efficiency explained between 3.3% and 24.7% of the PEV (N = from 59 to 193; Brendel et al. 2008).

The importance and organization of QTLs reflect the difficulty of the genetic selection. With several small-effect QTLs, genetic selection may be difficult due to a low response to selection (Barton and Keightley 2002). In our study, the result was contrary to our original hypothesis. The importance and organization of the detected QTLs was similar to that detected for phenology by Scotti-Saintagne et al. (2004), i.e., several QTLs with a small effect each in most chromosomes. This organization is different from that observed by Brendel et al. (2008) for water use efficiency, i.e., a few QTLs with a large effect. Especially for the QTLs of latent buds, compared with the two linked QTLs with 22% and 23% PEV, respectively, found on the same linkage group for apple tree (Segura et al. 2008), we detected six QTLs of nLBD with much lower PEVs (from 5.2% to 6.6%) and on several linkage groups. The species, age (3-year-old apple tree vs. 14-year-old oak), and contrast between alleles can explain this difference in terms of genetic architecture.

Conclusion and perspectives

Epicormic branch emergence is known to be under the control of both genetic and environmental effects, the latter including light exposure, water and nutrition resources, and the rejuvenation of the crown after damage (Jensen et al. 1997; Chaar and Colin 1999; Colin et al. 2010b; Meier et al. 2012). This study, based on the analysis of epicormic and sequential branching of an oak full-sib family, made it possible to investigate the genetic architecture of these traits through an internal observation of the stem wood by X-ray tomography. Our results revealed a moderate genetic effect on latent buds and epicormic branches and a limited and independent genetic control for the sequential branches. In addition, considering the numerous small-effect QTLs detected on most of the chromosomes, a genetic selection to reduce the sprouts and related defects seems difficult. However, some genomic regions were highlighted with hotspots of QTLs. We believe that the genetic control of buds and epicormic branches in these critical areas is related to some complex mechanisms such as axillary meristem initiation and bud dormancy. An in-depth study of the genetic architecture of branching traits would require the study of the stability of these QTLs and would refine their position using larger sample sizes and more environmental conditions. The oak genome sequence also provides a solid knowledge base necessary to decipher the physiological and molecular bases underlying branching trait variation in oak.

Acknowledgements J. Song received a PhD fellowship from the Jinan Bayle Wine Import Co. The experimental site was provided by UMR 1202 Biogeco (INRA-Univ. Bordeaux). The medical CT scanner was provided by UMR 1092 LERFoB (INRA-AgroParisTech). LERFoB is supported by a grant overseen by the French National Research Agency (ANR) as part of the "Investissements d'Avenir" program (ANR-11-LABX-0002-01, Lab of Excellence ARBRE). We warmly thank B. Garnier and C. Freyburger for the preparation of the CT scanning, JB. Morisset and P-A. Dherouville for their help with the interpretation of the scanned images, B. Dencausse, D. Rittié, and G. Maréchal for wood preparation, and F. Ehrenmann for data submission. We also thank P. Duba for an initial English revision.

References

Barton NH, Keightley PD (2002) Understanding quantitative genetic variation. Nat Rev Genet 3:11–21. doi:10.1038/nrg700

Beavis WD (1994) The power and deceit of QTL experiments: lessons from comparative QTL studies. Proc Forty-Ninth Annu Corn Sorghum Ind Res Conf 250–266

Bodénès C, Chancerel E, Ehrenmann F et al (2016) High-density linkage mapping and distribution of segregation distortion regions in the oak genome. DNA Res. doi:10.1093/dnares/dsw001

Bradshaw HD, Stettled RF (1995) Molecular genetics of growth and development in populus. Genetics 973:963–973

Brendel O, Thiec D, Scotti-Saintagne C et al (2008) Quantitative trait loci controlling water use efficiency and related traits in *Quercus robur* L. Tree Genet Genomes 4:263–278. doi:10.1007/s11295-007-0107-z

Chaar H, Colin F (1999) Impact of late frost on height growth in young sessile oak regenerations. Ann For Sci 56:417–429. doi:10.1051/forest:19990506

Chatfield SP, Stirnberg P, Forde BG, Leyser O (2000) The hormonal regulation of axillary bud growth in Arabidopsis. Plant J 24:159–169. doi:10.1046/j.1365-313X.2000.00862.x

Colin F, Ducousso A, Fontaine F (2010a) Epicormics in 13-year-old *Quercus petraea*: small effect of provenance and large influence of branches and growth unit limits. Ann For Sci 67:312–312. doi:10.1051/forest/2009118

Colin F, Fontaine F, Morisset JB, et al. (2012) Gourmands et bourgeons latents dans le bois. Conséquences pour la sylviculture. Forêts Fr. no. 550 39–41.

Colin F, Mothe F, Freyburger C et al (2010b) Tracking rameal traces in sessile oak trunks with X-ray computer tomography: biological bases, preliminary results and perspectives. Trees 24:953–967. doi:10.1007/s00468-010-0466-1

Colin F, Nicolas R, Jean-louis D, Fontaine F (2008) Initial spacing has little influence on transient epicormic shoots in a 20-year-old sessile oak plantation.

Conner PJ, Brown SK, Weeden NF (1998) Molecular-marker analysis of quantitative traits for growth and development in juvenile apple trees. Theor Appl Genet 96:1027–1035. doi:10.1007/s001220050835

Darvasi A, Soller M (1997) A simple method to calculate resolving power and confidence interval of QTL map location. Behav Genet 27:125–132

Epskamp S, Cramer AOJ, Waldorp LJ et al (2012) {qgraph}: network visualizations of relationships in psychometric data. J Stat Softw 48:1–18

Fabbrini F, Gaudet M, Bastien C et al (2012) Phenotypic plasticity, QTL mapping and genomic characterization of bud set in black poplar. BMC Plant Biol 12:47. doi:10.1186/1471-2229-12-47

Fontaine F, Kiefer E, Clément C et al (1999) Ontogeny of the proventitious epicormic buds in *Quercus petraea*. II. From 6 to 40 years of the tree's life. Trees 14:83–90. doi:10.1007/PL00009755

Fontaine F, Mothe F, Colin F, Duplat P (2004) Structural relationships between the epicormic formations on the trunk surface and defects induced in the wood of *Quercus petraea*. Trees - Struct Funct 18:295–306. doi:10.1007/s00468-003-0306-7

Forêts de France (2015) n°583 Mars

Freeman JS, Potts BM, Downes GM, et al. (2013) Stability of quantitative trait loci for growth and wood properties across multiple pedigrees and environments in *Eucalyptus globulus*. 1121–1134.

Frewen BE, Chen THH, Howe GT et al (2000) Quantitative trait loci and candidate gene mapping of bud set and bud flush in populus. Genetics 154:837–845

Freyburger C, Mothe F, Colin F, Fontaine F (2007) Exploitation d'images tomographiques RX pour l'analyse de la structure interne des gourmands de chêne. Procédure d'utilisation du plugin "Gourmands" avec ImageJ.

Gailing O, Langenfeld-Heyser R, Polle A, Finkeldey R (2008) Quantitative trait loci affecting stomatal density and growth in a *Quercus robur* progeny: implications for the adaptation to changing environments. Glob Chang Biol 14:1934–1946. doi:10.1111/j.1365-2486.2008.01621.x

Harmer R (1989) Some aspects of bud in young oak activity and branch formation. Ann des Sci For 46:217–219

Heuret P, Barthélémy D, Nicolini E, Atger C (2000) Analyse des composantes de la croissance en hauteur et de la formation du tronc chez le chêne sessile, *Quercus petraea* (Matt.) Liebl. (Fagaceae) en sylviculture dynamique. Can J Bot 78:361–373. doi:10.1139/b00-012

IGN (2013) La France par zonage écoforestier.

Jensen JS, Wellendorf H, Jager K et al (1997) Analysis of a 17-year old dutch open-pollinated progeny trial with *Quercus robur* (l.). For Genet 4:139–147

Kao CH, Zeng ZB, Teasdale RD (1999) Multiple interval mapping for quantitative trait loci. Genetics 152:1203–1216

Korol AB, Ronin YI, Nevo E, Hayes PM (1998) Multi-interval mapping of correlated trait complexes. 80:273–284

Leyser O (2009) The control of shoot branching: an example of plant information processing. Plant Cell Environ 32:694–703. doi:10.1111/j.1365-3040.2009.01930.x

McSteen P, Leyser O (2005) Shoot branching. Annu Rev Plant Biol 56:353–374. doi:10.1146/annurev.arplant.56.032604.144122

Meadows JS, Burkhardt EC (2001) Epicormic branches affect lumber grade and value in willow oak. South J Appl For 25:136–141

Meier A, Saunders MR (2013) Assessing internal epicormic dynamics in *Quercus alba* L. using CT scanning: the strong effects of shoot development and tree growth relative to progeny level genetic variation. Trees 27:865–877. doi:10.1007/s00468-013-0840-x

Meier AR, Saunders MR, Michler CH (2012) Epicormic buds in trees: a review of bud establishment, development and dormancy release. Tree Physiol 32:565–584. doi:10.1093/treephys/tps040

Morisset JB (2012) Tomographie à rayons X; analyse et modélisation de l'ontogénèse des épicormiques du chêne sessile (*Quercus petraea* (L.) Matt.).

Morisset JB, Mothe F, Bock J et al (2012a) Epicormic ontogeny in *Quercus petraea* constrains the highly plausible control of epicormic sprouting by water and carbohydrates. Ann Bot 109:365–377. doi:10.1093/aob/mcr292

Morisset JB, Mothe F, Colin F (2012b) Observation of *Quercus petraea* epicormics with X-ray CT reveals strong pith-to-bark correlations: Silvicultural and ecological implications. For Ecol Manag 278:127–137. doi:10.1016/j.foreco.2012.05.015

Nicolini E, Barthélémy D, Heuret P (2000) Influence de la densité du couvert forestier sur le développement architectural de jeunes chênes sessiles, *Quercus petraea* (Matt.) Liebl. (Fagaceae), en régénération forestière. Can J Bot 78:1531–1544. doi:10.1139/b00-125

Parelle J, Zapater M, Scotti-Saintagne C et al (2007) Quantitative trait loci of tolerance to waterlogging in a European oak (*Quercus robur* L.): physiological relevance and temporal effect patterns. Plant Cell Environ 30:422–434. doi:10.1111/j.1365-3040.2006.01629.x

Plomion C, Aury J, Elle JO et al (2016) Decoding the oak genome : public release of sequence data, assembly, annotation and publication strategies. Mol Ecol Resour 16:254–265. doi:10.1111/1755-0998.12425

R Core Team (2015) R: a language and environment for statistical computing. R Found Stat Comput Vienna, Austria doi: ISBN 3-900051-07-0,

Saintagne C, Bodénès C, Barreneche T et al (2004) Distribution of genomic regions differentiating oak species assessed by QTL detection. Heredity (Edinb) 92:20–30. doi:10.1038/sj.hdy.6800358

Savill PS, Kanowski P (1993) Tree improvement programs for European oaks: goals and strategies. Ann Des Sci For 50:368s–383s. doi:10.1051/forest:19930741

Scalfi M, Troggio M, Piovani P et al (2004) A RAPD, AFLP and SSR linkage map, and QTL analysis in European beech (*Fagus sylvatica* L.). Theor Appl Genet 108:433–441. doi:10.1007/s00122-003-1461-3

Scotti-Saintagne C, Bertocchi E, Barreneche T et al (2005) Quantitative trait loci mapping for vegetative propagation in pedunculate oak. Ann For Sci 62:369–374. doi:10.1051/forest

Scotti-Saintagne C, Bodénès C, Barreneche T et al (2004) Detection of quantitative trait loci controlling bud burst and height growth in *Quercus robur* L. Theor Appl Genet 109:1648–1659. doi:10.1007/s00122-004-1789-3

Segura V, Durel C-E, Costes E (2008) Dissecting apple tree architecture into genetic, ontogenetic and environmental effects: QTL mapping. Tree Genet Genomes 5:165–179. doi:10.1007/s11295-008-0181-x

Shepherd M, Cross M, Dieters MJ, Henry R (2002) Branch architecture QTL for *Pinus elliottii* var. *elliottii* × *Pinus caribaea* var. *hondurensis* hybrids. Ann For Sci 59:617–625. doi:10.1051/forest

Socquet-Juglard D, Christen D, Devènes G et al (2012) Mapping architectural, phenological, and fruit quality QTLs in apricot. Plant Mol Biol Report 31:387–397. doi:10.1007/s11105-012-0511-x

Sosnowski O, Charcosset A, Joets J (2012) Biomercator V3: an upgrade of genetic map compilation and quantitative trait loci meta-analysis algorithms. Bioinformatics 28:2082–2083. doi:10.1093/bioinformatics/bts313

Teichmann T, Muhr M (2015) Shaping plant architecture. Front Plant Sci 6:1–18. doi:10.3389/fpls.2015.00233

Voorrips RE (2002) Computer note MapChart: software for the graphical presentation of linkage maps and QTLs. J Hered 93:77–78

Wu RL (1998) Genetic mapping of QTLs affecting tree growth and architecture in populus: implication for ideotype breeding. Theor Appl Genet 96:447–457. doi:10.1007/s001220050761

Zhang D, Zhang Z, Yang K (2006) QTL analysis of growth and wood chemical content traits in an interspecific backcross family of white poplar (*Populus tomentosa* × *P-bolleana*) × *P*-tomentosa. Can J For Res Can Rech For 36:2015–2023. doi:10.1139/x06-103

Data archiving statement

The genetic maps are available in Quercus Portal:

http://w3.pierroton.inra.fr/QuercusPortal/

CMap Comparative Map Viewer for female parental LGs:

http://w3.pierroton.inra.fr/cgi-bin/cmap/viewer?mapMenu=&featureMenu=&corrMenu=&displayMenu=&advancedMenu=&ref_map_accs=-1&ref_map_start=&ref_map_stop=&ft_SNP=2&ft_DEFAULT=2&sub=Draw+selected+maps&prev_ref_species_acc=2&prev_ref_map_accs=&ref_map_set_acc=44&ref_species_acc=2&data_source=CMAP+OAK+DATABASE

CMap Comparative Map Viewer for male parental LGs:

http://w3.pierroton.inra.fr/cgi-bin/cmap/viewer?mapMenu=&featureMenu=&corrMenu=&displayMenu=&advancedMenu=&ref_map_accs=-1&ref_map_start=&ref_map_stop=&ft_SNP=2&ft_DEFAULT=2&sub=Draw+selected+maps&prev_ref_species_acc=2&prev_ref_map_accs=&ref_map_set_acc=44&ref_species_acc=2&data_source=CMAP+OAK+DATABASE

The phenotypic measurements were submitted in QuercusMap: https://w3.pierroton.inra.fr/QuercusPortal/index.php?p=qmap

2.2 Conclusions sur l'analyse QTL de la ramification du chêne observée par tomographie à rayon X

La tomographie à rayon X a permis d'observer les traces de bougeons et les nœuds des branches épicormiques et séquentielles à l'intérieur du bois, même si elles ont déjà arrêté leur développement et ont été englobées dans le tronc. Cette observation nous permet de quantifier et créer les traits de la ramification plus complets par rapport à ceux observés à l'extérieur du bois. Une architecture génétique des différents types de rameaux a été mise en évidence. En effet, nous avons trouvé des régions génomiques intéressantes et des contrôles génétiques de la ramification épicormique qui sont probablement liés aux mécanismes de l'initiation du méristème axillaire et de la dormance du bourgeon.

Dans cette étude, nous supposons que le contrôle génétique de la branche séquentielle est indépendant et relativement faible. Le nombre de branches séquentielles par mètre (nSeqBC=33,9) est beaucoup plus élevé que celui rapporté dans l'étude de Morisset (2012) chez le chêne sessile et l'étude de Meier and Saunders (2013) chez le chêne blanc (environ 20 branches séquentielle par mètre). Cette différence inattendue peut être liée aux différentes espèces de chêne étudiés. Les arbres que nous avons mesurés sont relativement jeunes par rapport aux études précédentes (14 ans vs. 28-55 ans), par conséquent, une branche épicormique qui ont été initiée par une trace de bourgeon latent très courte a pu été enregistrée comme une branche séquentielle durant l'interprétation d'image scannée.

Le temps de l'interprétation des images scannées reste critique, dix mois d'interprétation manuelle sur plus de 200.000 images scannées. Ceci est très long, surtout pour une analyse QTL qui a besoin de plus d'échantillons pour augmenter la puissance de détection.

Nous pouvons alors nous demander quel est l'impact de la méthode d'observation sur notre analyse QTL de la ramification. Si nous utilisons une méthode d'observation plus rapide et non destructive sur les même génotypes dans le même site, les QTLs seraient-ils les mêmes que ceux étudiés par tomographie à rayon X ?

Nous avons confirmé que le contrôle génétique reste modéré pour la ramification épicormique par rapport à l'effet environnement. Des génotypes identiques réagissent-ils

différemment sur la ramification épicormique dans deux environnements très différents? Est-ce que le nombre des QTLs et le pourcentage de la variance expliqué par QTLs détectés sont stables en utilisant l'observation à l'extérieur des troncs des mêmes génotypes dans deux environnements différents? La localisation des nouveaux QTLs détectés sera-t-elle proche ou superposée à celle des QTLs dans cette étude ?